Supporting Information

Breaking the lattice match of Pd on Au(111) nanowires: manipulating the island and epitaxial growth pathways to boost oxygen reduction reactivity

Jingchun Wang, Xiaoyu Qiu, Keying Su, Siyuan Wang, Jiatian Li, and Yawen Tang**

Jiangsu Key Laboratory of New Power Batteries, Jiangsu Collaborative Innovation Center of Biomedical Functional Materials, School of Chemistry and Materials Science, Nanjing Normal University, Nanjing 210023, China.

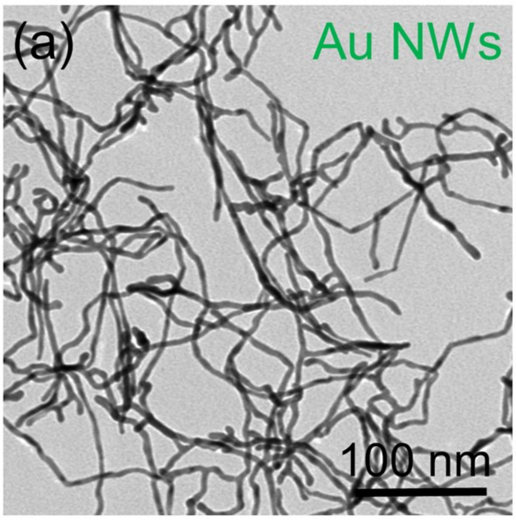

Fig. S1 TEM image of the newly-prepared Au NWs as seed.

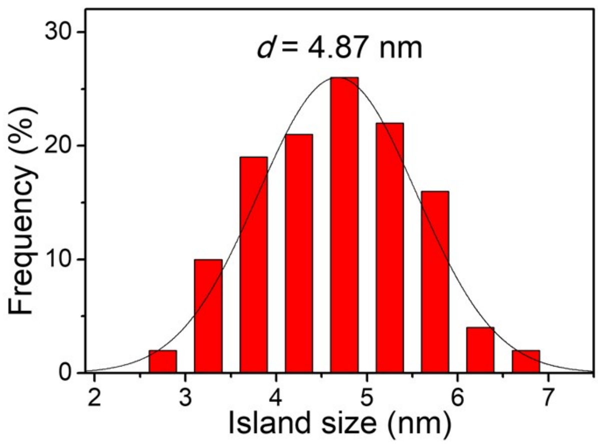

Fig. S2 Histogram of size distribution of Pd islands on VW Au@Pd HNWs.

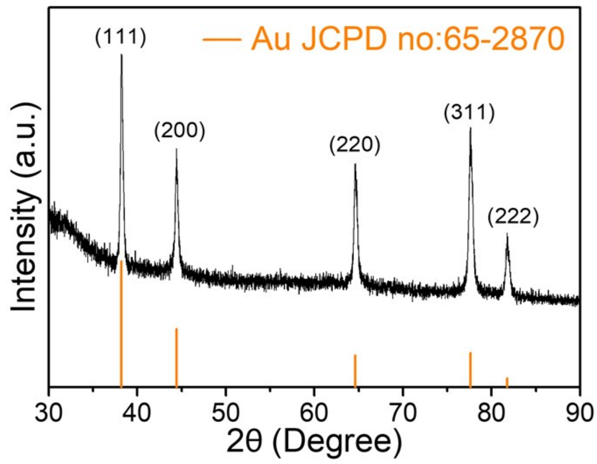

Fig. S3 XRD pattern of pure Au NWs.

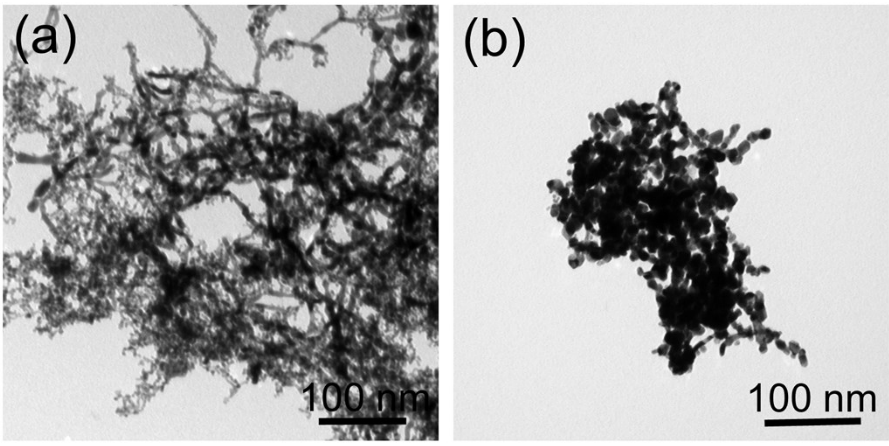

Fig. S4 TEM images of the products prepared in the absence of PDDA at the pH value of (a) 5 and (b) 11.

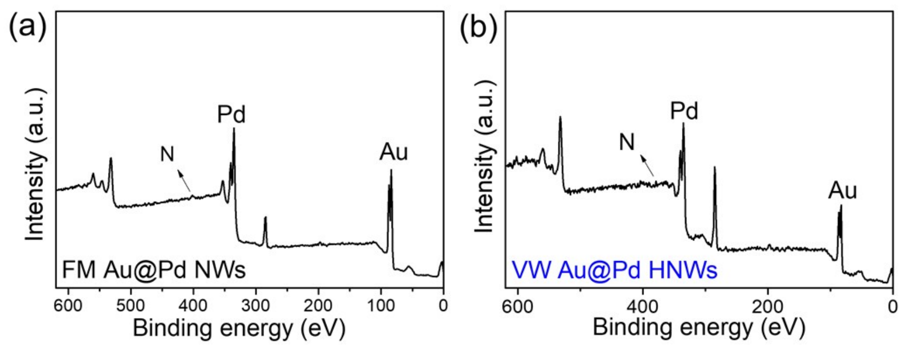

Fig. S5 Full XPS survey spectrum of the (a) VW Au@Pd HNWs and (b) FM Au@Pd NWs.

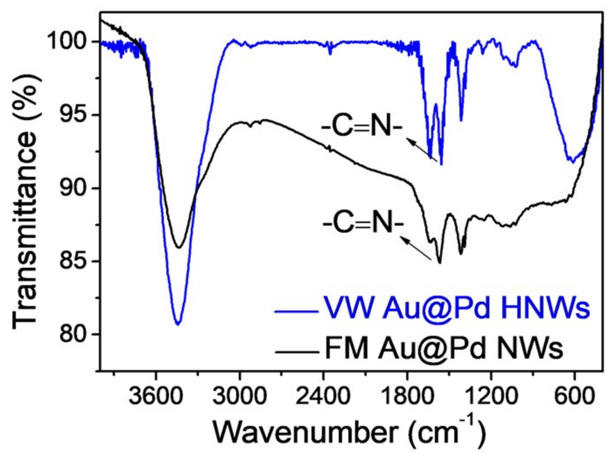

Fig. S6 FTIR spectrum of the FM Au@Pd NWs and VW Au@Pd HNWs.

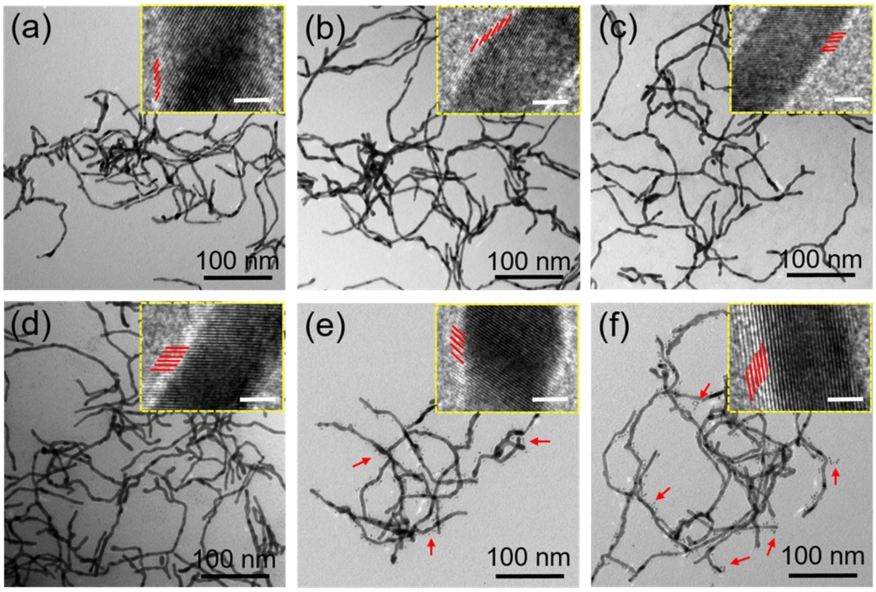

Fig. S7 Representative TEM images of products using different dosage of K_2PdCl_4 at the pH value of 5. (a) 0.125 mL, (b) 0.5 mL, (c) 1 mL, (d) 1.5 mL, (e) 2mL and (f) 3 mL. Insert: HRTEM images of products showing the relevant shell thickness. The insert scale bar is 2 nm.

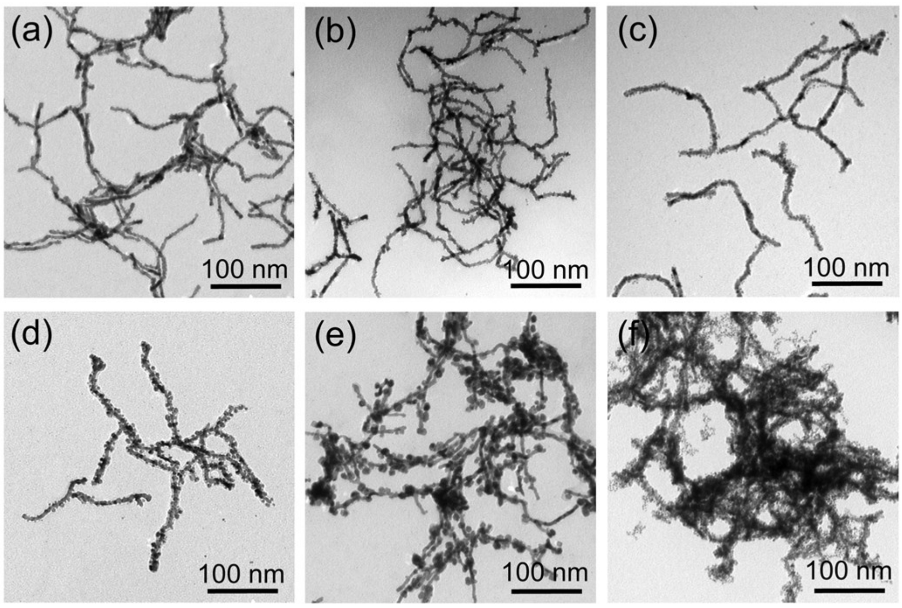

Fig. S8 Representative TEM images of products using different dosage of K_2PdCl_4 at the pH value of 11. (a) 0.125 mL, (b) 0.5 mL, (c) 1 mL, (d) 1.5 mL, (e) 2mL and (f) 3 mL.

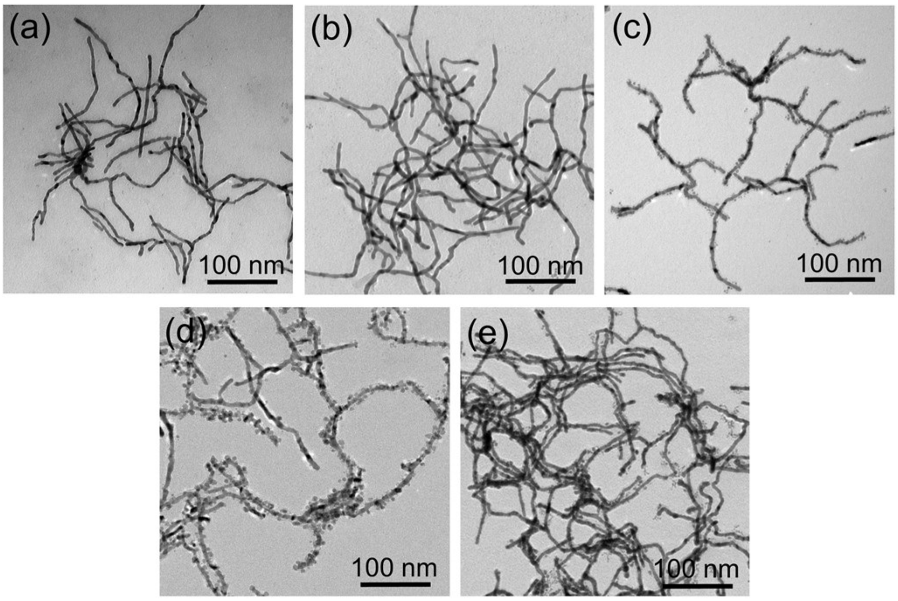

Fig. S9 Representative TEM images of products obtained at different pH values. (a) 5, (b) 7, (c) 9, (d) 11 and (e) 13.

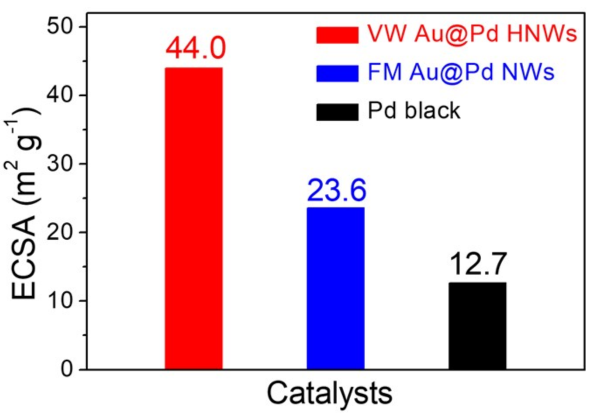

Fig. S10 ECSA Histogram of VW Au@Pd HNWs, FM Au@Pd NWs and Pd black.

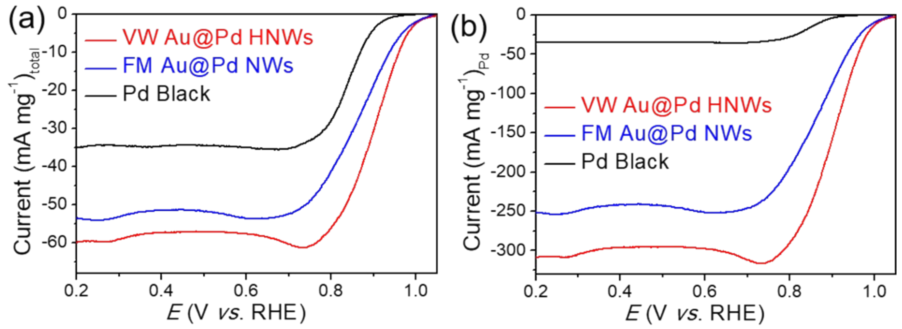

Fig. S11 ORR polarization curves showing the mass activity of the VW Au@Pd HNWs, FM Au@Pd NWs and Pd black. (a) Total mass activity, (b) mass activity normalized to Pd.

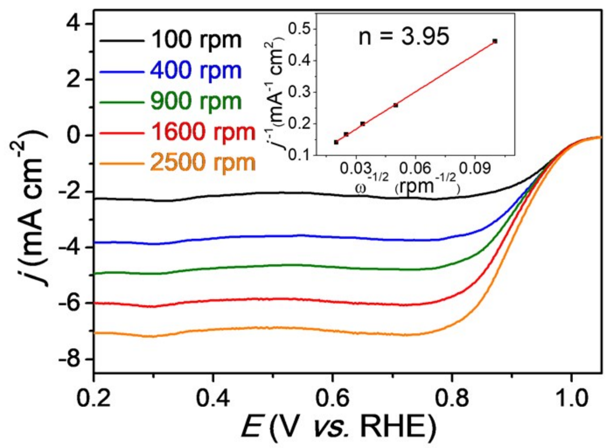

Fig. S12 ORR polarization curves of VW Au@Pd HNWs in O_2-saturated 0.1 M KOH solution at different rotation rates, insert: Koutecky-Levich plot (j^{-1} *vs*. $\omega^{-1/2}$) at 0.60 V.

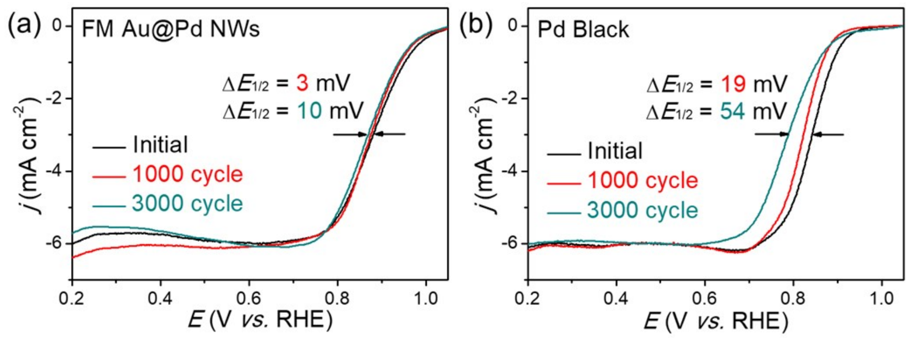

Fig. S13 ORR polarization curves of the (a) FM Au@Pd NWs and (b) Pd black before and after ADTs in O_2-saturated 0.1 M KOH solution at a scan rate of 5 mV s^{-1}.

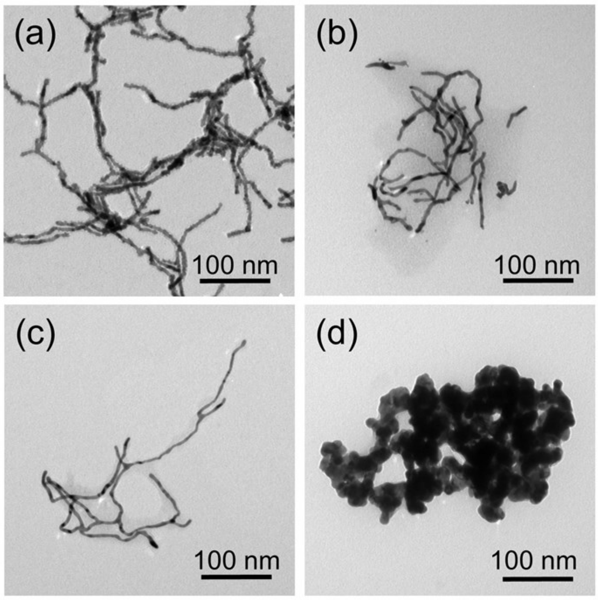

Fig. S14 TEM images of (a) VW Au@Pd HNWs, (b) FM Au@Pd NWs, (c) Au NWs and (d) Pd black after ADTs.

Table S1 Comparison of the ORR performance of VW Au@Pd HNWs and FM Au@Pd NWs with some state-of-the-art catalysts in 0.1 M KOH solution.

Number	Catalysts	E_{onset} (V *vs.* RHE)	$E_{1/2}$ (V *vs.* RHE)	ORR mass activity (at 0.9 V, mA mg^{-1})	Reference
1	VW Au@Pd HNWs	1.070	0.910	32.4 $_{(total)}$, 171.0 $_{(Pd)}$	This work
2	FM Au@Pd NWs	1.042	0.880	19.1 $_{(total)}$, 92.0 $_{(Pd)}$	This work
3	Au@Pd nanoparticles	~ 0.950	0.833	~ 18.0 $_{(total)}$	*J. Am. Chem. Soc.* 2018, 140, 8918-8923
4	AuPdCo/C-intermetallic	~0.975	~0.850	~ 10.0 $_{(total)}$	*Nat. Commun.* 2014, 5, 5185
5	PdMo bimetallene/C	~1.050	0.95	~16.4 $_{(total)}$	*Nature*, 2019, 574, 81-85
6	Au@PtPd mesoporous nanorod	1.010	0.920	~ 69.0 $_{(Pd)}$	*ACS Appl. Energy Mater.* 2018, 1, 4891-4898
7	Pd/Au NWs	~0.890	0.796	~ 30.0$_{(Pd)}$	*Chem. Eur. J.* 2020, 26, 4019-4024
8	$Au/Cu_{40}Pd_{60}$ NPs	~1.042	~0.892	~ 140 $_{(Pd)}$	*J. Am. Chem. Soc.* 2014, 136, 15026-15033
9	Au-O-PdZn	~0.980	~0.900	105 $_{(Pd)}$	*ACS Nano* 2019, 13, 5968-5974
10	Pd@Pt core-conformal shell NCs	~0.990	0.850	260$_{(Pd)}$	*Nanoscale*, 2016,8, 1698-1703